ESTCP
Cost and Performance Report

(UX-0126)

Applications of Synthetic Aperture Radar (SAR) to UXO Delineation

May 2004

ENVIRONMENTAL SECURITY
TECHNOLOGY CERTIFICATION PROGRAM

U.S. Department of Defense

COST & PERFORMANCE REPORT
ESTCP Project: UX-0126

TABLE OF CONTENTS

Page

TABLE OF CONTENTS (continued)

Page

FIGURES

TABLES

ACRONYMS AND ABBREVIATIONS

ARL	Army Research Laboratory
ATD	Advanced Technology Demonstration
ATL	Advanced Technology Demonstration
BDU	bomb dummy unit
CECOM RDEC I2WD	Communications-Electronics Command Research, Development & Engineering Center Intelligence & Information Warfare Directorate
dB	decibel
DARPA	Defense Advanced Research Projects Agency
DGPS	differential global positioning systems
DoD	Department of Defense
ERDC	Engineer Research and Development Center
ESTCP	Environmental Security Technology Certification Program
FOPEN	foliage penetration
GPS	global positioning system
GSL	Geotechnical and Structures Laboratory
HH	copolarized; both transmitted and received signal are horizontally polarized
HV	crosspolarized; transmitted signal horizontally polarized, received signal vertically polarized
ITAR	International Traffic in Arms Regulations
MIT/LL	Massachusetts Institute of Technology Lincoln Laboratory
MLFMA	Multi-level Fast Multipole Algorithm
MoM	method of moments
PWF	polarimetric whitening filter
QC/QA	quality control/quality assurance
RCS	radar cross section
RF	radio frequency
RFI	radio frequency interference
SAR	synthetic aperture radar

T/C	peak target to mean clutter ratio
UHF	ultra high frequency
UWB	ultrawide-band
UXO	unexploded ordnance
VHF	very high frequency
VV	copolarized; both transmitted and received signal vertically polarized

ACKNOWLEDGEMENTS

The U.S. Army Engineer Research and Development Center (ERDC), Geotechnical and Structures Laboratory (GSL), was responsible for coordinating the efforts of the Massachusetts Institute of Technology Lincoln Laboratory (MIT/LL), Army Research Laboratory (ARL), and Duke University. MIT/LL performed quality control/quality assurance (QC/QA) on the data provided by Lockheed Martin, developers of the foliage penetration (FOPEN) synthetic aperture radar (SAR) system, and also processed the data to generate imagery used in the modeling efforts. The algorithms used to simulate SAR scattering from individual UXO were developed by Duke. These algorithms were employed by ARL to generate SAR imagery to model the signatures of unexploded ordnance (UXO). The ERDC produced this report.

This project was supported by the Environmental Security Technology Certification Program (ESTCP).

The technical information in this report is extracted from the final reports provided by the project participants. No raw or processed imagery is included in this report because of the International Traffic in Arms Regulation (ITAR) classification of the data. The final report of each participant was submitted to ESTCP under separate cover [1, 2, 3]. Those reports that contain imagery ([1] and [3]) are not approved for release without permission from Defense Advanced Research Projects Agency (DARPA). The final project report [4] does not contain imagery and is available for public release.

Technical material contained in this report has been approved for public release.

1.0 EXECUTIVE SUMMARY

The clearing of areas contaminated with unexploded ordnance (UXO) is the Army's highest priority Environmental Restoration problem. The Department of Defense (DoD) currently spends millions of dollars annually on UXO cleanup efforts. Initial evaluation of a UXO contaminated area involves the review of historical documents, surface walkovers of randomly chosen areas, and statistical modeling to estimate the ordnance in place. Presently, there are no efficient and cost-effective means of estimating the extent of contamination at UXO sites. The foliage penetration (FOPEN) synthetic aperture radar (SAR) involved in an Advanced Technology Demonstration (ATD) funded by Defense Advanced Research Projects Agency (DARPA) has the potential for delineating ordnance impact areas at a fraction of the time and cost incurred using current methods and technology.

The FOPEN SAR is an ultrawide-band (UWB) system that uses low frequencies to achieve foliage penetration. The system has a very high frequency (VHF) frequency range of approximately 20-70 MHz and ultra high frequency (UHF) range of approximately 200-500 MHz. Its basic operating principle involves transmitting of pulsed radio frequency waves and receiving the echoes scattered from targets and the ground surface. The echoes are subjected to analog preprocessing, digitized, and further digitally processed to produce the final imagery. The UHF band is a fully polarimetric (HH[1], VV[2], HV[3]) side-looking radar. The VHF band operates with HH polarization.

A test grid containing three target sizes was established to determine the feasibility of using the FOPEN SAR to delineate UXO ranges. The targets were 155-mm projectiles and objects representing 500- and 2,000-lb bombs. Each type of target was arranged in grids of sparse, moderate, and dense arrays in an open field with low ground cover. Some targets were placed under trees. No targets were buried because of environmental restrictions on Camp Navajo, Arizona.

The demonstration's primary objective was measuring UXO target signatures in various settings, the secondary was determining whether the FOPEN SAR has applications for UXO range delineation. The FOPEN system is capable of imaging the larger targets in the sparse array in the open field. The 155-mm projects are clearly observable as a cluster in the imagery in dense arrays in the open field. None of the targets located under trees appears to be visible in the images. The FOPEN SAR is capable of delineating UXO in benign environments where large concentrated ordnance is present on the surface. No measurements were done to assess capabilities against buried targets.

Since this work was an add-on to a DARPA sponsored project, there was no direct involvement with regulatory issues.

---

[1] Copolarized—Both transmitted and received signal are horizontally polarized.
[2] Copolarized—Both transmitted and received signal are vertically polarized.
[3] Cross-polarized—Transmitted signal is horizontally polarized, received signal is vertically polarized.

This page left blank intentionally.

2.0 TECHNOLOGY DESCRIPTION

2.1 TECHNOLOGY DEVELOPMENT AND APPLICATION

The resolution of a radar antenna is dependent on the antenna aperture—the larger the antenna, the better the resolution. A SAR takes advantage of motion of the antenna to achieve an apparent antenna length, or aperture, greater than its actual length. As the antenna moves along a flight path, successive echoes are received from the same target and may be processed to give spatial resolution equivalent to an antenna as long as the distance the antenna moved when receiving the target echoes. Thus, the terminology "synthetic aperture radar" is used to describe the radar system.

Atmospheric conditions such as clouds and rain do not significantly degrade the SAR signal. However, the presence of foliage (trees, brush, grasses) can greatly attenuate the signal. The foliage penetration (FOPEN) SAR is an ultrawide-band system that uses lower frequencies to "see" through the foliage and achieve foliage penetration. Its basic operating principle involves transmitting pulsed radio frequency waves and receiving echoes scattered from targets and the ground surface. The echoes are subjected to analog preprocessing, digitized, and further digitally processed to produce the final imagery.

The system is operated in one of two modes—spot or strip. In spot mode, the radar is focused on a single point and data are gathered at different angles as the aircraft flies over the area. An image 3 km by 3 km is typically obtained in spot mode. Strip mode differs from spot mode in that the radar viewing angle is held fixed and a swath of ground is imaged along the flight path. Strip mode produces a 2 km by 7 km image. Image resolution varies but is typically less than 1 m in the UHF band for both modes. The data acquired during this test were collected in strip mode.

The UHF band of the FOPEN SAR is a fully polarimetric (HH, VV, HV) side-looking radar. Although the exact operating parameters cannot be given, a general range is given below. It was designed primarily for the detection of large vehicles under foliage. This project investigated its feasibility for delineating UXO ranges. Specifically, 155-mm projectiles and items that simulated 500-lb and 2,000-lb bombs were placed on the ground surface and under foliage. The imagery was analyzed to determine if the signatures from UXO clusters and individual UXO could be separated from the background noise and clutter, i.e., anything not a UXO.

	Frequency Range	Integration Angle	Resolution
VHF	20–70 MHz	40º to 50º	< 10 m
UHF	200–500 MHz	30º to 40º	< 1 m

2.2 PROCESS DESCRIPTION

Acquisition of the imagery required coordination with DARPA, through Communications-Electronics Command Research, Development and Engineering Center Intelligence and Information Warfare Directorate (CECOM RDEC I2WD), to schedule a flight of the FOPEN SAR system. It was necessary to submit a flight plan specifying the area of coverage, number of passes and their headings, depression angle, type of data to be collected (e.g., VHF, UHF,

differential global positioning system [DGPS]), and deliverables (e.g., raw radar data, navigation data, imagery, and test report describing the data collection).

2.3 PREVIOUS TESTING OF THE TECHNOLOGY

No prior test data is available.

2.4 ADVANTAGES AND LIMITATIONS

The primary advantage of using an airborne-based system is the ability to acquire a large amount of data covering a wide area in a relatively short period of time. Current methods for estimating the extent of a UXO-contaminated site are multiphase efforts, ground-based, and the site evaluation generally requires several weeks or months. With the airborne SAR, the time frame could be reduced to days. Although the FOPEN SAR system can rapidly gather data over a large area, it was designed to detect large tactical vehicles and its resolution limits the size of UXO that can be detected. Ordnance are typically found in clusters within the primary radius of a firing range, and a cluster of smaller UXO, which are not detectable individually, may be imaged. However, on the fringes of a range where the distribution of UXO is sparse, only the larger ordnance may be detected.

3.0 DEMONSTRATION DESIGN

3.1 PERFORMANCE OBJECTIVES

The performance objective was to measure UXO target signatures in varying target placement conditions. The placement conditions include target orientation, proximity to other targets, and foliage coverage. Three sizes of UXO were measured: 2,000-lb bomb, 500-lb bomb, and 155-mm projectile. A bomb dummy unit (BDU) was used to simulate the 2,000-lb bomb whereas the 500-lb bomb was represented by the front section of a BDU. The targets were placed on the ground surface in grids ranging from a high density of UXO to only one item. These target and clutter data were compared to electromagnetic model data generated using the same UXO placement and Camp Navajo soil parameters.

The decibel (dB) level of the target signature is an acceptable criterion for measuring success of the performance objective. If the UXO signature was measurably greater than background levels, then the overall objective was deemed a success. The FOPEN SAR was successful in imaging the larger targets, both in clusters and individually, placed on the ground surface in the open field. The 155-mm projectiles were detectable in clusters with less than a projectile length between projectiles. Both the larger and smaller targets were not discernible from background noise and clutter when placed under foliage. The FOPEN SAR is not recommended for use on sites with significant foliage cover. However, other SAR systems designed specifically for detecting ordnance-size objects may prove to be more successful than the FOPEN system.

3.2 SELECTION OF TEST SITE

This work was an add-on to the primary project funded by DARPA involving the development of a FOPEN SAR system; therefore, the project was not involved with selecting the demonstration site at Camp Navajo, Arizona. Concerns for the FOPEN SAR include unrestricted flight paths, minimum radio frequency (RF) interference, roads covered by a foliage canopy, roads accessible to large vehicles, and a large area consisting of both open field and tree cover for calibration purposes. In addition to site accessibility, site characteristics desirable for a SAR system specifically designed for UXO detection are low-loss soil for maximum signal penetration; areas having long, short and no vegetation; tree covered areas; burial of items allowed; and a UXO firing range on the installation or availability of inert UXO at or near the installation.

The installation, Camp Navajo, has stringent restrictions on any digging operations so no items were buried. This limited evaluation of the FOPEN SAR to the detection of surface and foliage covered items. No definitive statements on its ability to detect subsurface items can be made.

3.3 TEST SITE/FACILITY HISTORY/CHARACTERISTICS

Camp Navajo is currently a National Guard training site and munitions storage depot operated by the Arizona National Guard. It is in the town of Bellemont within Coconino County, Arizona, approximately 8 miles northwest of Flagstaff. Before its original establishment as the Navajo

Ordnance Depot in 1942, the area was used primarily for sheep and cattle ranching and the timber industry.

Items stored on the installation and available for use included 155-mm projectiles and BDUs, both full and front sections. The calibration and open field aim point is located in the northwest region of Camp Navajo (Figure 1). Within the aim point, an area approximately 400 m by 100 m was selected for the UXO test site (Figure 2). Figure 3 provides a panoramic view of the area within the aim point chosen for the test site. Large open spaces were available to establish the test grid with isolated trees within the grid and clusters of trees along the southern border available for foliage cover.

3.4 PHYSICAL SET-UP AND OPERATION

During a presite visit (May 7, 2001) and when the test grid was established, soil samples were collected for laboratory testing and analyzed to determine the conductivity and dielectric permittivity properties of the soil. These parameters were later used in generating synthetic imagery for modeling purposes.

Establishment of the UXO test plot was accomplished in two days, July 9 and 10, 2001. The grid encompassed an area approximately 300 m x 75 m (Figure 4). Five grid areas were established, three of which contained different arrangements of the 155-mm projectile, 500-lb target, and 2,000-lb target. One area was a random arrangement of UXO and miscellaneous metal, and another was an arrangement of the three ordnance types placed under trees. The 155-mm grid consisted of five 5 m x 5 m subsections with the density of ordnance ranging from 1 to 54 projectiles per subsection. The 500-lb target grid contained three 5 m x 5 m subsections whereas three 10 m x 10 m subsections were used for the 2,000-lb targets. The randomly arranged grid was 10 m x 10 m and contained three 155-mm projectiles, several lengths of rebar, aluminum vent pipe, metal plates, and razor wire.

All grid subsections were oriented north-south and sufficiently spaced to avoid image interference between sections. Camp Navajo personnel assisted with transportation of the ordnance to the test grid and placement of the ordnance in the grids. A flatbed truck was required to haul to the site the large number of items emplaced, and a forklift was used to initially place the ordnance in the grid subsections. After the ordnance were on the ground, they were manually shifted to their final positions. Ground truth data collection involved surveying the location of each target and the collection of ground and aerial photographs of UXO deployment sites.

Calibration targets were used as control points for the UXO flight data. The 23 targets deployed included triangular trihedrals, triangular dihedrals, and square trihedrals. The data acquisition flight was flown on July 18, 2001.

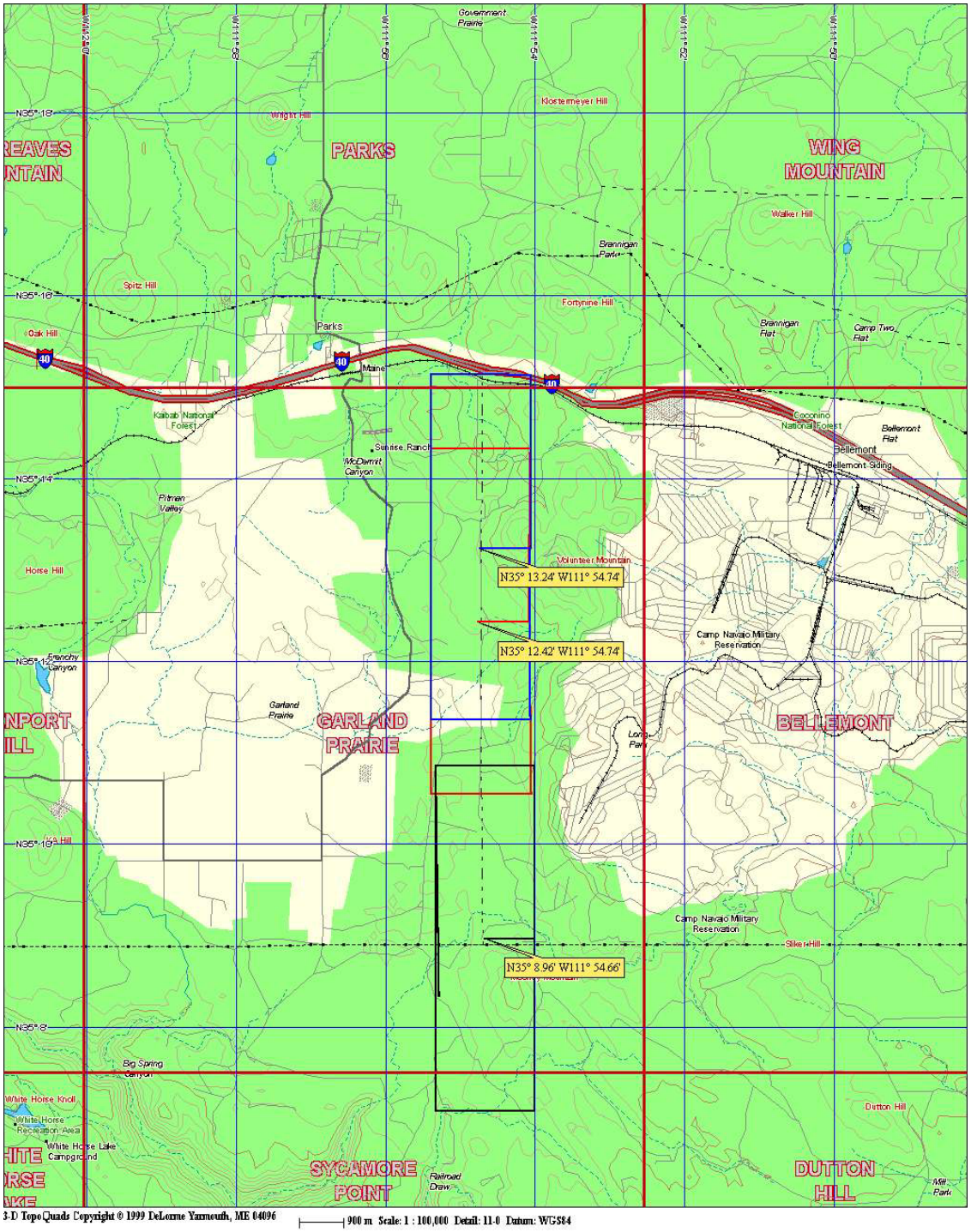

Figure 1. Location of Calibration and Open Field Aim Point on Camp Navajo, Arizona.

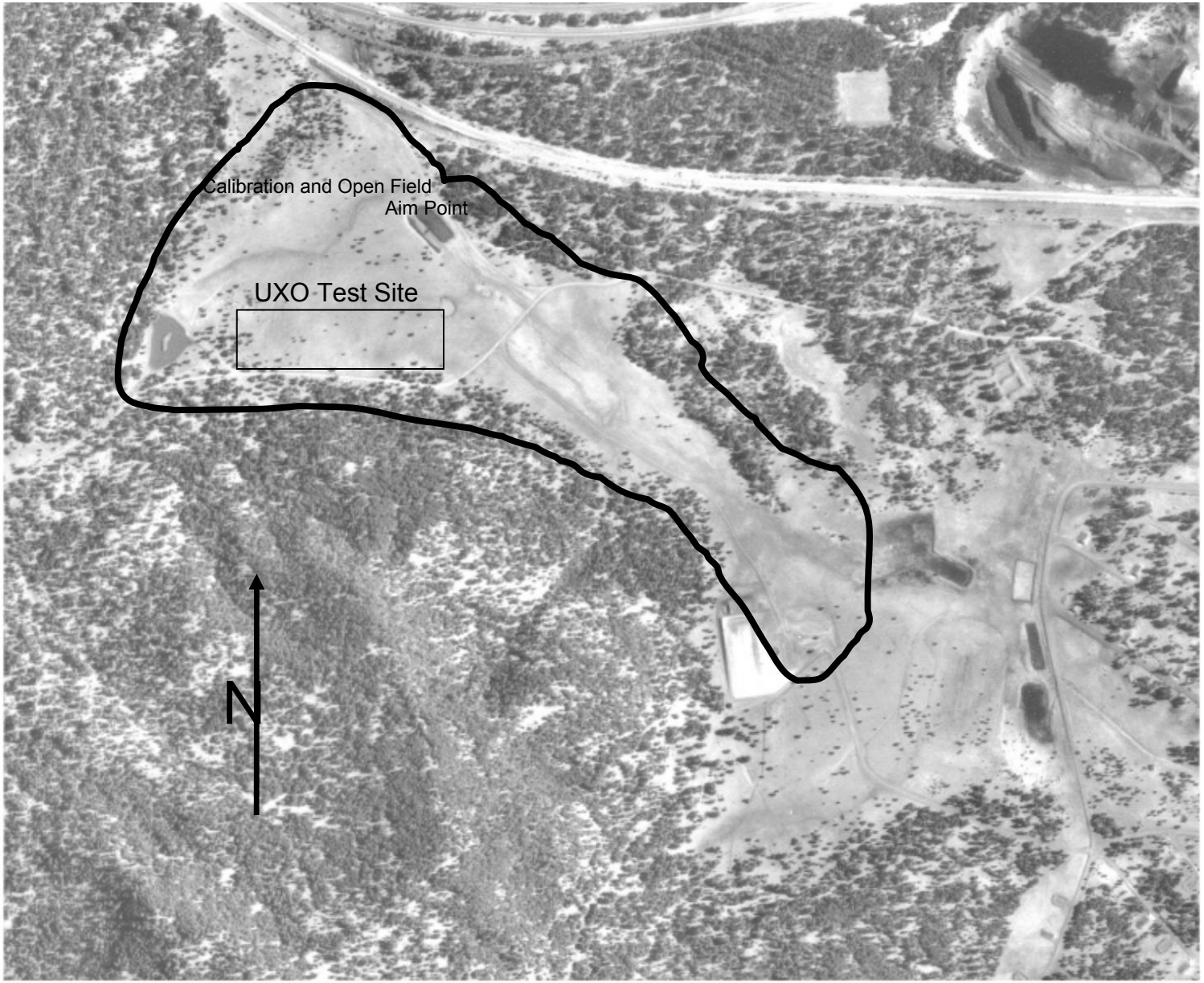

Figure 2. General Location of the UXO Test Grid Within the Calibration and Open Field Aim Point.

Figure 3. Panoramic View of UXO Test Site. (View is west to east.)

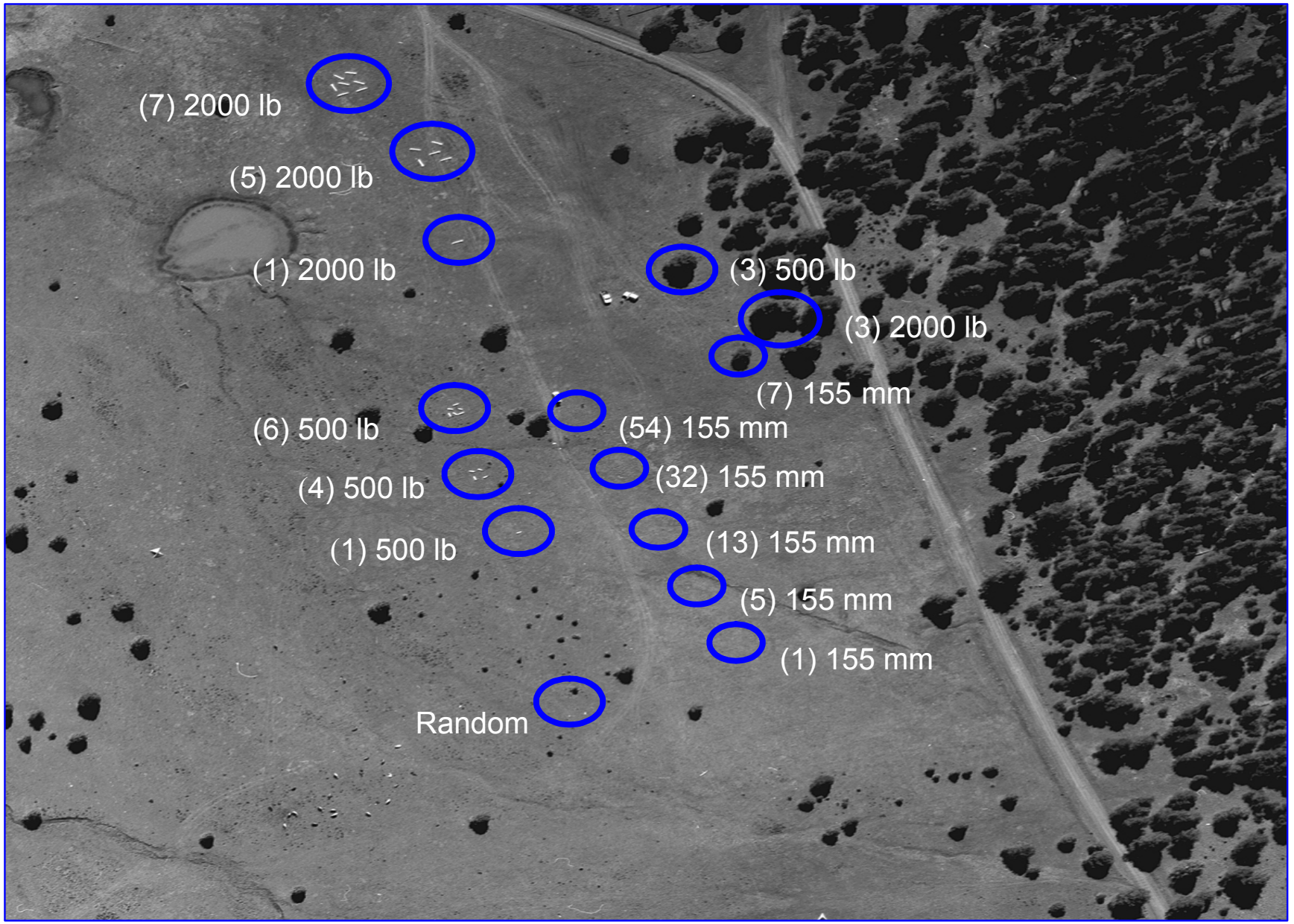

Figure 4. Aerial Photograph of UXO Test Grid and Placement of UXO.
(Numbers in parentheses indicate the number of ordnance in a subsection.)

3.5 ANALYTICAL PROCEDURES

3.5.1 Image Processing

MIT Lincoln Laboratory (MIT/LL) images were formed by a fast backprojection technique [5] that provides better image focus for aircraft flight that is not perfectly straight. With backprojection processing, perfect focus is possible across the entire image regardless of the aircraft off-track motion error. Image formation of VHF and UHF SAR data using the fast backprojection algorithm includes radio frequency interference (RFI) rejection, height of focus correction, and calibration. Five data passes were collected over the UXO test area. Preliminary processing was done on all five passes to determine candidate passes for final processing. Preliminary processing used RFI rejection software, version 1 (a single binary filter formed from the center of the pass and applied to the entire pass), aircraft position data generated from the autonomous global positioning system (GPS) and internal navigation system, and no height of focus correction. As planned, final processing was completed on two passes. Final processing included RFI rejection software, version 2 (a bank of binary filters generated across the entire pass and applied to the pulses from which it was generated), aircraft position data generated from differential GPS, height of focus correction, and calibration. A slight improvement in image quality (better focus and reduced residual RFI) is seen in the final images when compared with the preliminary images.

3.5.2 Data Modeling

Duke University developed a mesh-generation package for general UXO shapes and used this model to represent the targets subsequently modeled by the Army Research Laboratory (ARL). Figure 5 depicts the meshes used to represent the 155-mm, 500-lb bomb, and 2,000-lb bomb (BDU-38B-2000). The triangular patch models require a large number of triangles, N, to appropriately model each target, with the tradeoff being accuracy of the modeling versus the amount of memory (related to N^2) and computer time (related to N^3) necessary to evaluate each model. The models used here are reasonable representations of intact UXO but do not include the effects of fins. One of the important issues to be examined involved the applicability of linearity in the context of SAR scattering from multiple UXO. Duke considered this issue in detail by extending its multilevel fast multipole algorithm (MLFMA) software for modeling an arbitrary number of UXO in the presence of soil. An iterative formulation was developed to model the SAR signature of multiple UXO. Assume for simplicity there are two UXO, UXO1 and UXO2, although the procedure developed is applicable to an arbitrary number of targets. First compute the currents induced on targets UXO1 and UXO2 in isolation caused by the fields incident from the sensor (and no interactions *between* the targets). In the next step, the fields incident on UXO1 are represented as the incident fields from the sensor plus the scattered fields from UXO2, where, to compute the latter, the induced currents on UXO2 from the first step are used. This yields an updated version of the currents induced on UXO1; the currents on UXO2 are updated similarly. This process repeats iteratively until the induced currents converge for both targets. The number of iterations required is dictated by the amount of coupling between the two targets.

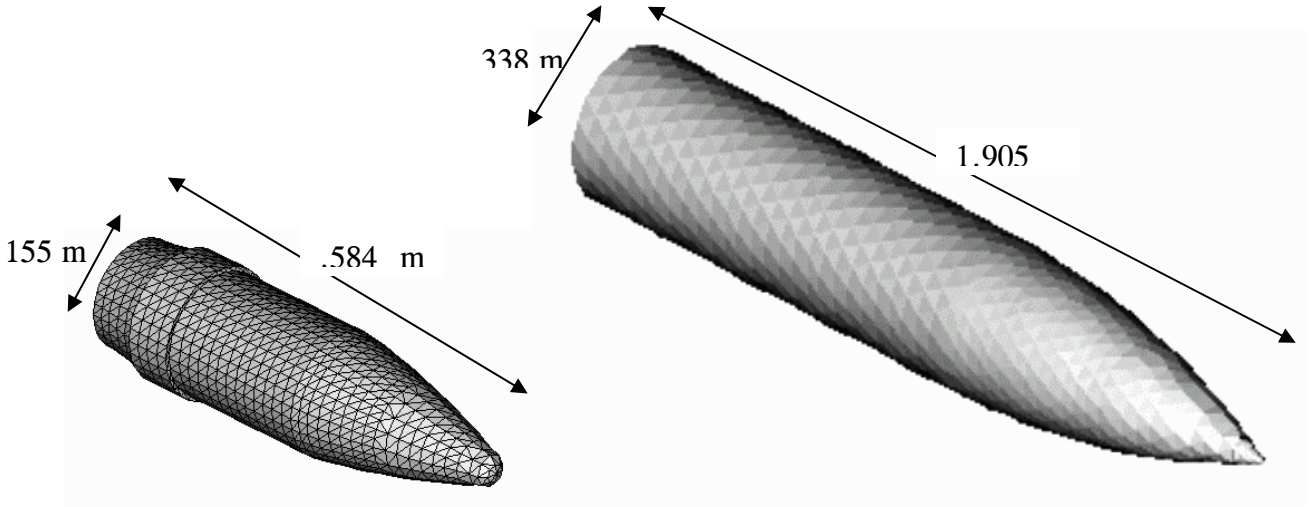

155-mm model (left) and 500-lb bomb model (right)

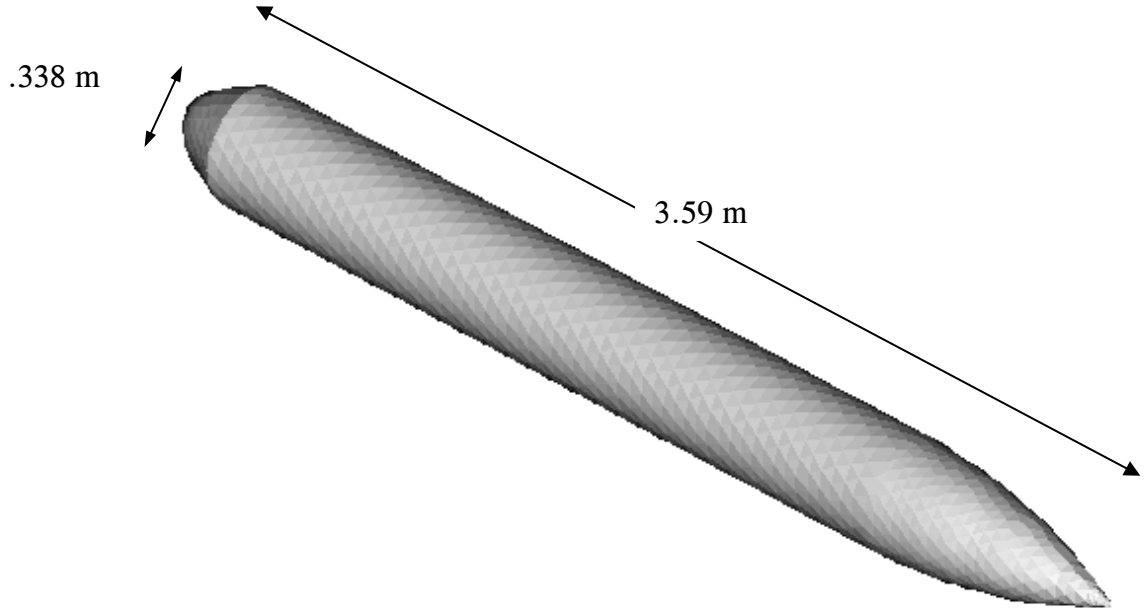

2,000-lb bomb model (BDU-38B-2000) (not to scale)

Figure 5. Triangular Patch Meshes Used to Model the UXO.

Figure 6 depicts the mesh used to simulate scattering from two unexploded ordnance (UXO) buried in soil, using soil properties characterized by complex dielectric constant ε_r=5-*j*0.2 and conductivity $\sigma = 0.01$ S/m. The incident angles (see coordinate system in Figure 6) are θ_i=60° and φ_i=120°, and the bistatic scattering angles are θ_s=60° and $-180^\circ \le \varphi_s \le 180^\circ$. For this example, two sets of results are considered: (1) the radar cross section (RCS) computed rigorously, via the iterative formulation discussed above and (2) the RCS computed by treating each UXO in isolation and simply adding their signatures (ignoring interaction). The latter approach is expected to yield reasonable results because the interaction effects are diminished by propagation through the lossy ground. The RCS results in Figure 7, for operation at 600 MHz, indicate that the simple linear combination (no interactions) model can predict the general RCS variation with angle, although the detailed RCS can be off by several dB. In this example N_1=N_2=8,295.

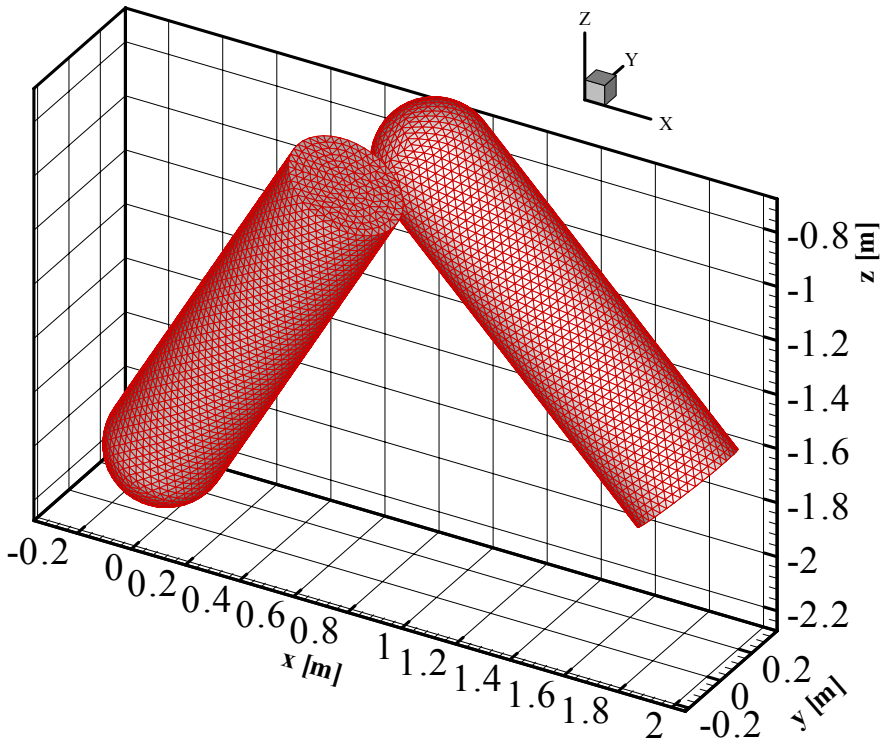

Figure 6. Mesh Used to Model Scattering from Two UXO Buried in Soil.
(The soil interface is at z = 0.)

The results in Figure 7 indicate that simple linear addition of the individual target signatures, ignoring inter-target wave interaction, yields excellent agreement with the rigorous solution, in which all interactions are accounted for. Consequently, in ARL's comparisons, they have ignored inter-target interactions. The two UXO in Figure 6 and Figure 7 are relatively closely situated. The model demonstrates the expected reduced coupling as the targets are further separated.

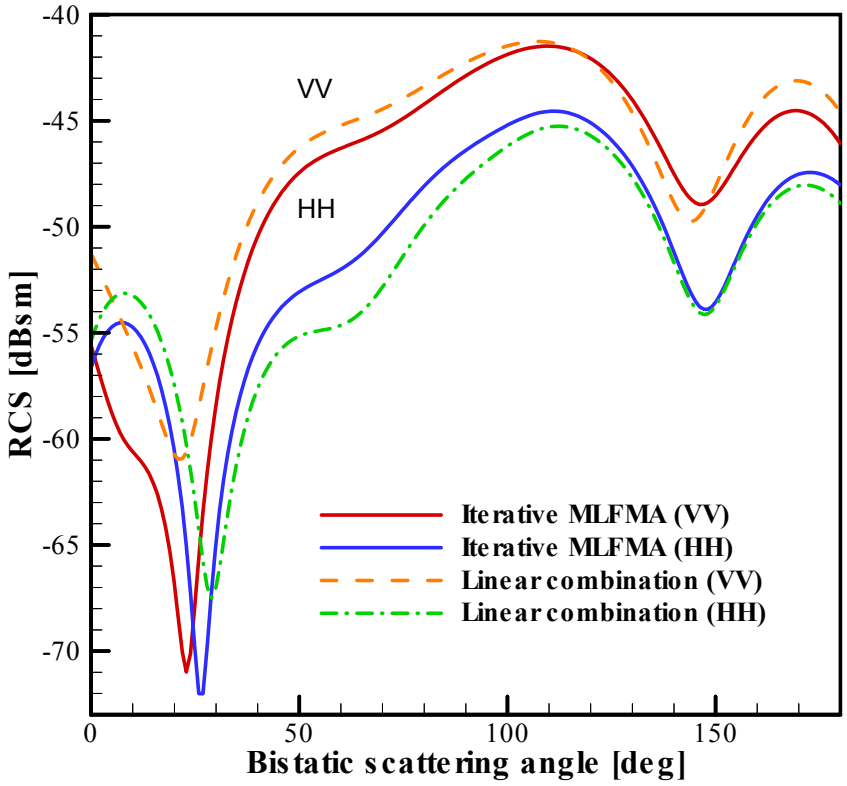

Figure 7. Bistatic RCS for the Problem Depicted in Figure 6, at 600 MHz. (Results are shown when all interactions are accounted for via the algorithm [MLFMA] discussed above, and when the targets are modeled in isolation and simply added.)

ARL took the data from the UXO passes and converted it for use in their in-house UWB data quality and focusing programs [3]. The method of moments (MoM) modeling technique was used for this analysis. MoM models are based on a full-wave formulation of Maxwell's equations and show great promise for detailed 3-D analysis of reasonable size targets across a wide frequency range. Electrically large bodies (targets) require many triangular patches to accurately model the surface currents on the body. Once the current has been calculated, the scattered fields and the RCS can be found directly. MoM codes require regular size triangles appropriate for the smallest region to be represented (typically 1/10 of a wavelength). Duke University provided the triangular patch models for the test targets.

4.0 PERFORMANCE ASSESSMENT

4.1 PERFORMANCE DATA

It was generally thought that the 2,000-lb bomb-size targets could be detected in the open field by the bandwidth used by the FOPEN SAR system. However, resolution of the system was questionable for the smaller targets and no capability was shown for any targets hidden beneath foliage.

4.1.1 Imagery—MIT/LL

2,000-lb Bomb Deployment. Figure 8 shows an example cross-range cut through the peak pixel of the UHF HH and VV polarization images of the dense 2,000-lb bomb deployment for an aircraft heading of 0^{o}. The cut passes through the two visible 2,000-lb bombs; the arrows indicate the length of the 2,000-lb bomb. The peak dB level measured over the targets is at least 10 dB above the local clutter, suggesting that the targets should be detectable. The image statistics for the 2,000-lb bomb dense deployment with polarimetric whitening filter (PWF) applied are summarized in Table 1. The 2,000-lb target dense deployment peak target is twice the clutter standard deviation or more above the mean clutter under these surface conditions. Table 2 lists the peak RCS statistics for all the 2,000-lb bomb deployments at both aircraft headings. The variation in RCS with aspect is observed in the sparse deployment. The sparse deployment contained a single target oriented 0°, and the peak RCS at that heading is considerably greater than at 30°. The dense and medium deployments both had targets oriented at approximately 0° and 30° so similar values of peak RCS are measured. Hence, having *multilook capability would probably improve UXO detection*.

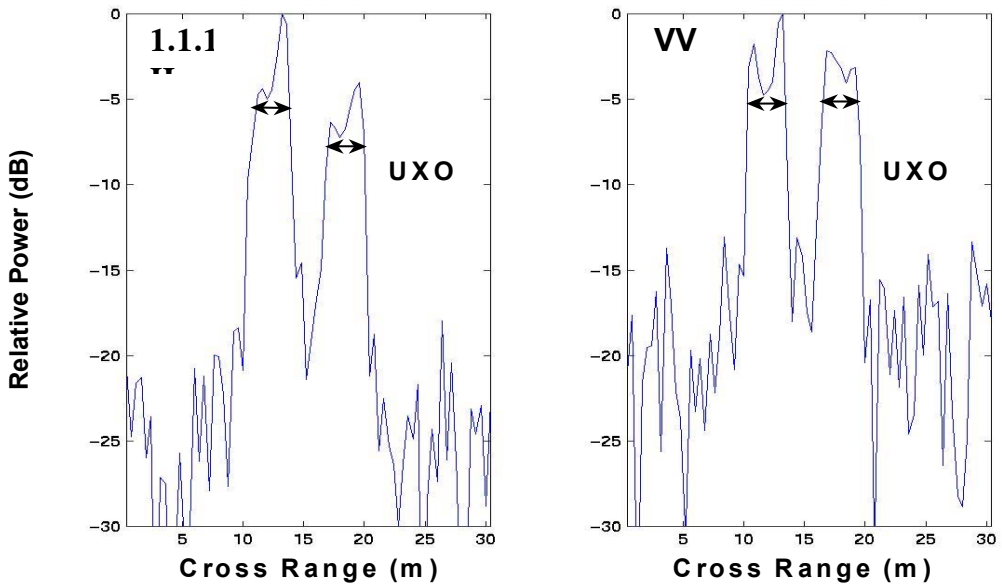

Figure 8. UHF Cross-Range Cut Through UXOs from 0° Aircraft Heading Image, 2,000-lb Bomb Dense Deployment.

Table 1. 2,000-lb Bomb Dense Deployment Peak RCS Statistics for HH, VV, and PWF Data.

	Peak RCS (dBsm)	T/C (dB)	Clutter Standard Deviation
HH[1]	5.2	26.9	5.9
HV[2]	−12.5	18.3	5.8
VV[3]	0.4	25.0	6.1
PWF	12.0	21.3	3.1

Table 2. Peak RCS (dBsm) for 2,000-lb Bomb Open Deployments, Aircraft Headings 0° and 30°.

	HH	VV	HV
Dense (7)			
0°	5.7	1.1	−9.6
30°	5.2	0.4	−12.5
Medium (5)			
0°	6.4	0.3	−9.9
30°	5.2	0.9	−9.4
Sparse (1)			
0°	5.7	−3.3	−11.5
30°	1.9	−8.6	−9.3

For the VHF HH polarization images of the 2,000-lb bomb dense deployment, the peak pixel RCS for the 0° aircraft heading is −2.7 dBsm, resulting in a peak target to mean clutter ratio (T/C) of 12.4 dB. The peak pixel RCS for the 30° aircraft heading is −4.7 dBsm, resulting in a T/C of 9.0 dB. The grass backscatter standard deviation is about 5 dB; therefore, *detection of the UXO deployments in this test is expected to be difficult with the VHF data*.

500-lb Bomb Deployment. The peak pixel RCS of the 500-lb bomb for the 0° aircraft heading is 1.8 dBsm (HH) and −4.4 dBsm (VV), resulting in a T/C of 23.0 dB (HH) and 20.0 dB (VV). The peak pixel RCS of the 500-lb bomb for the 30° aircraft heading is −0.1 dBsm (HH) and −5.6 dBsm (VV), resulting in a T/C of 21.6 dB (HH) and 19.4 dB (VV). Cross-range cuts through the peak pixel of the UHF HH and VV polarization images of the 500-lb bomb deployment for an aircraft heading of 0° are shown in Figure 9. Arrows indicate the position of the UXO. Since the peak RCS is at least 10 dB above the peak local clutter, the 500-lb targets should be detectable under this scenario. Table 3 summarizes the peak RCS statistics for the various 500-lb bomb deployments. Similar behavior is observed relative to aspect angle as was seen with the 2,000-lb targets.

[1] Copolarized—Both transmitted and received signal are horizontally polarized.
[2] Cross-polarized—Transmitted signal is horizontally polarized, received signal is vertically polarized.
[3] Copolarized—Both transmitted and received signal are vertically polarized.

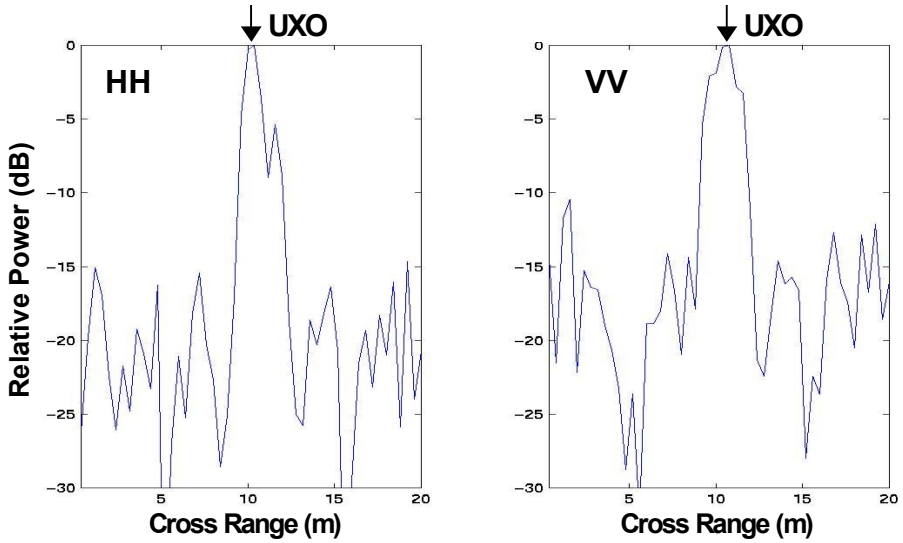

Figure 9. UHF Cross-Range Cut Through UXO from 0° Aircraft Heading Image, 500-lb Bomb Deployment.

Table 3. Peak RCS (dBsm) for 500-lb Bomb Open Deployments.

	HH	VV	HV
Dense (6)			
0°	1.8	– 4.4	– 8.8
30°	–0.1	– 5.6	–14.6
Medium (4)			
0°	1.4	– 2.0	–14.2
30°	2.5	– 6.0	–10.1
Sparse (1)			
0°	0.4	– 4.5	–18.0
30°	–5.9	–13.2	–19.2

155-mm Projectile Deployment. The peak pixel RCS of the 155-mm projectile for the 0° aircraft heading was −3.8 dBsm (HH) and −3.4 dBsm (VV), resulting in a T/C of 18.0 dB (HH) and 20.9 dB (VV). The peak pixel RCS of the 155-mm projectile for the 30° aircraft heading was −5.0 dBsm (HH) and −1.2 dBsm (VV), resulting in a T/C of 17.0 dB (HH) and 23.3 dB (VV). Cross-range cuts through the cluster peak of the UHF HH and VV polarization images of the 155-mm projectile deployment for an aircraft heading of 0° are shown in Figure 10. The image statistics for the 155-mm projectile deployment are provided in Table 4 and Table 5. The T/C is two to four times greater than the clutter standard deviation for each polarization, six times for PWF, suggesting that the dense arrangement of 155-mm is detectable. However, the clutter background level is higher (Figure 10) than that for the 2,000-lb target (Figure 8) and 500-lb target (Figure 9) so further analysis is required to determine if the 155-mm dense arrangement would be distinguishable from false alarm sources. Note that in Table 7 the peak RCS values are

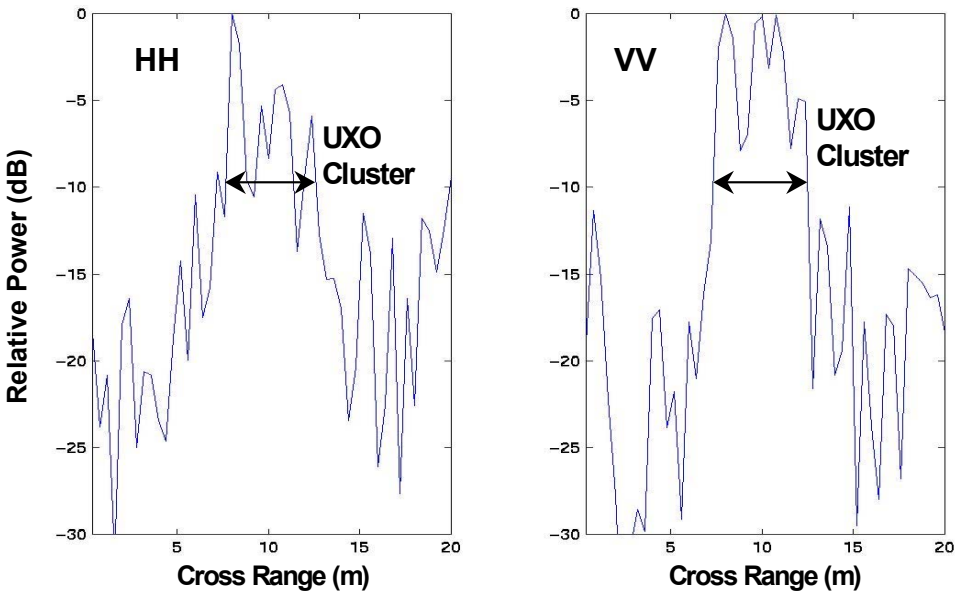

Figure 10. UHF Cross-Range Cut Through UXO Cluster 0° Aircraft Heading Image, 155-mm Projectile Deployment.

Table 4. 155-mm Projectile Peak RCS Statistics for HH, HV, VV, and PWF Data.

	Peak RCS (dBsm)	T/C (dB)	Clutter Standard Deviation
HH	− 5.0	17.0	5.4
HV	−16.5	13.7	5.7
VV	− 1.2	23.3	5.5
PWF	9.0	18.0	3.1

Table 5. Peak RCS (dBsm) for 155-mm Projectile Open Deployments Aircraft Headings 0° and 30°.

Deployment (Number in Cluster)	HH	VV	HV
Dense (54)			
0°	−3.8	−3.4	−14.9
30°	−5.0	−1.2	−16.5
Medium (32)			
0°	−6.9	−5.7	−15.8
30°	−5.6	−5.7	−16.0
Sparse (13)			
0°	−7.2	−6.6	−18.1
30°	−9.7	−9.3	−18.6
Sparse (5)			
0°	−6.9	−7.7	−19.9
30°	−8.4	−9.3	−20.0
Sparse (1)			
0°	− 9.9	−10.6	−20.2
30°	−11.7	−13.5	−19.4

similar for both aircraft headings for the sparse deployment containing a single target (oriented at 0°). This indicates that the background clutter provides a similar level of response as a single 155-mm, so the smaller targets will probably be detectable only in large groupings.

UXO Deployment Under Trees. Only slight differences in the images are visible between the images acquired prior to placement of the UXO under foliage and after deployment. Those differences are seen in the VV polarization image of the 155-mm projectiles where a few of the projectiles are not under the tree cover. For UXO in the open but with tree clutter nearby, the T/C could drop by 10-12 dB, since the mean tree RCS is approximately 10-12 dB above the mean RCS of the grass. In addition, the RCS of a UXO under trees could drop on average by another 10 dB because of the two-way foliage attenuation at UHF. Hence, based on the available data, *detection of UXO targets that are concealed by trees does not look promising using the FOPEN ATD SAR*.

4.1.2 Data Modeling—Electromagnetic Modeling (Army Research Laboratory [ARL])

The models assume a flat, completely isotropic ground beneath the target with no surface or subsurface irregularities or nearby clutter to perturb the imagery. The model also does not include any noise or interference the radars may receive (internally or externally generated). In addition, the models, being analytic in nature, do not exhibit any errors in image formation due to unsensed motion or acceleration that might be present in actual radars. This makes these images very "clean" looking compared to those from actual radars, which might suffer from any or all of the above perturbations to the data. Thus, these results will allow us to understand if the UXO exhibit unique frequency or aspect angle-dependent radar scattering behavior that would permit the discrimination of the UXO from clutter objects.

The narrow frequency bandwidth, which translates to a loss in range resolution, of the FOPEN UHF waveform makes it difficult to resolve the direction of oblique angled targets and an overlapping of target signatures. The loss of resolution means it will be extremely difficult to separate the returns from individual UXO in a collection of UXO, and difficult to separate UXO returns from those due to naturally occurring clutter (trees, large rocks, etc.).

The strength of the image response is dependent on the aspect angle of the radar signal with the target. The strongest response occurs when the target is broadside to the radar viewing angle. It is possible that this feature may be exploited to distinguish targets from naturally occurring clutter.

Cylindrical shaped targets, such as UXO, tend to have the largest response in copolarized channels (HH and VV). The largest return in the HH image comes from a broadside target, whereas end-on targets are brighter in the VV channel. The cross-polarized response (HV) is always weaker than either of the copolarized responses. The oblique targets are the brightest in the cross-pol images because the cross-pol highlights the asymmetry of the targets.

4.2 PERFORMANCE CRITERIA

The peak RCS and clutter standard deviation were used to evaluate the FOPEN SAR system for detecting UXO. A PWF process [6] was applied to the data. PWF reduces the clutter standard deviation and often improves detection performance. Peak RCS can fluctuate due to calibration variation pass-to-pass. The T/C (10*log [peak target to mean local clutter ratio]) removes any pass-to-pass calibration. The larger the clutter standard deviation, the more false alarms obtained. Depending on the distribution of the clutter and the number of false alarms that could be tolerated, generally the peak target should be $2\sigma_c$ (twice the clutter standard deviation) or more above the mean clutter ($T/C > 2\sigma_c$) for reliable detection. The peak RCS occurs on different UXO for each aircraft heading, and generally on a target oriented in a direction similar to the aircraft heading. By comparing the RCS values over the different target densities, it is possible to see the variation in RCS with aspect.

4.3 DATA ASSESSMENT

4.3.1 Imagery

[1] The initial results of the FOPEN ATD UHF imagery from the UXO *open* deployments are encouraging. Both the 2,000-lb and 500-lb items are visible in the HH and VV polarization channels when the UXO orientation is parallel to the aircraft heading. Combining multiple-look angles improves detection of the 2,000- and 500-lb items. A T/C ratio greater than 20 dB in the dense deployments enabled detection of the UXO against the grass background. It may be possible to detect all targets with a lower T/C threshold; however other objects (trees, bushes, fences, etc.) would also be detected. It would be necessary to employ a discrimination stage (for example, a stage that looks for groups of detections with a certain minimum density that would signify a UXO impact area) to reduce detection of false alarms. Clusters of 155-mm projectiles are visible in the VV polarization data. The clutter background appears to have more influence on these smaller targets. *None of the targets, even the larger 2,000-lb bomb size, was detectable under foliage.* For UXO proximate to trees, the T/C could drop 10-12 dB and, if under trees, another 10 dB decrease is expected. The VHF data were found to be limited in UXO detection in this experiment due to insufficient resolution and the small RCS of the UXO targets at this frequency band. The FOPEN ATD UHF data were found to be limited by multiplicative noise due to spectral notching, which makes the detection of the dimmer UXO targets difficult.

4.3.2 Modeling

The modeling studies by ARL started before MIT/LL completed the image processing, so ARL did not know which passes MIT/LL would eventually select for further processing. The images processed by MIT/LL span less than 40° in azimuth. Figure 11 shows plots of calculated RCS over a 40° range for the 2,000-lb, 500-lb, and 155-mm target (Personal communication, November 25, 2002, Anders Sullivan, Electronics Engineer, Army Research Laboratory, Adelphi, Maryland). The 155-mm curve exhibits little-to-moderate variation whereas the 500-lb and 2,000-lb curves vary significantly. The average RCS computed from each curve in Figure 11 (using the center frequency of the UHF portion of the FOPEN radar) is compared to the measured (MIT/LL) RCS in Table 6. Assuming the MIT/LL data are perfectly calibrated,

uncertainties in the soil relative dielectric permittivity and target orientation relative to the flight path of the radar most likely account for the 4- to 5-dB discrepancy between the measured and modeled data. It is important to note that because the heading offset between the 0° and 30° flights and the integration angle (less than 40°) do not sum to greater than 90°, it is not certain

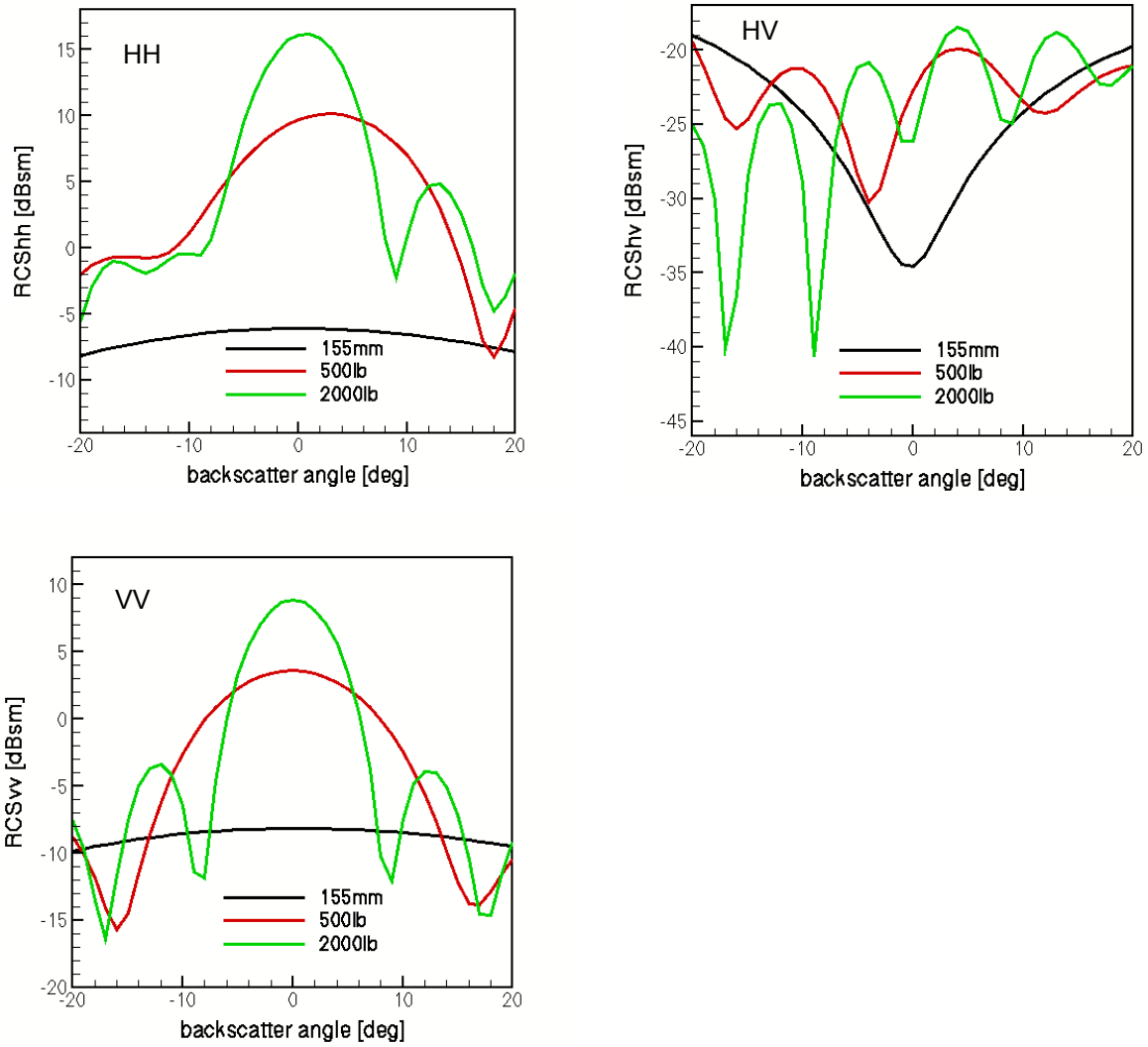

Figure 11. RCS of 155-mm Shell, 500-lb Bomb, and 2,000-lb Bomb as a Function of Azimuth Angle.

Table 6. Comparison of Measured and Modeled Average RCS over Notional 40° Azimuth Range.

	155-mm projectile		500-lb bomb		2,000-lb bomb	
	Measured	**Model**	**Measured**	**Model**	**Measured**	**Model**
HH	- 9.9	- 6.7	0.4	5.9	5.7	9.4
HV	-19.4	-23.2	-18.0	-22.4	-11.5	-22.4
VV	-10.6	- 8.6	- 4.5	- 0.7	- 3.3	2.0

that the target was imaged broadside. To illustrate the importance of target orientation relative to the radar flight path, assume that there was a 20° heading offset so that the MIT/LL image was not formed evenly around the target broadside. (See Figure 12.) In this case, the RCS would be averaged over -40° to 0° in azimuth. The average RCS values for this scenario are given in Table 7. The MIT/LL measurement values and the previous model averages are also given. The 20° heading offset is indicated by the "-40:0" label in the table, and the previous nonoffset average is given by the "-20:20" label. As can be seen, the offset model results are closer to the MIT/LL measured data. This suggests that the image data are not purely broadside to the target and that the SAR models, given the uncertainties in the measurements, are representative of the radar system.

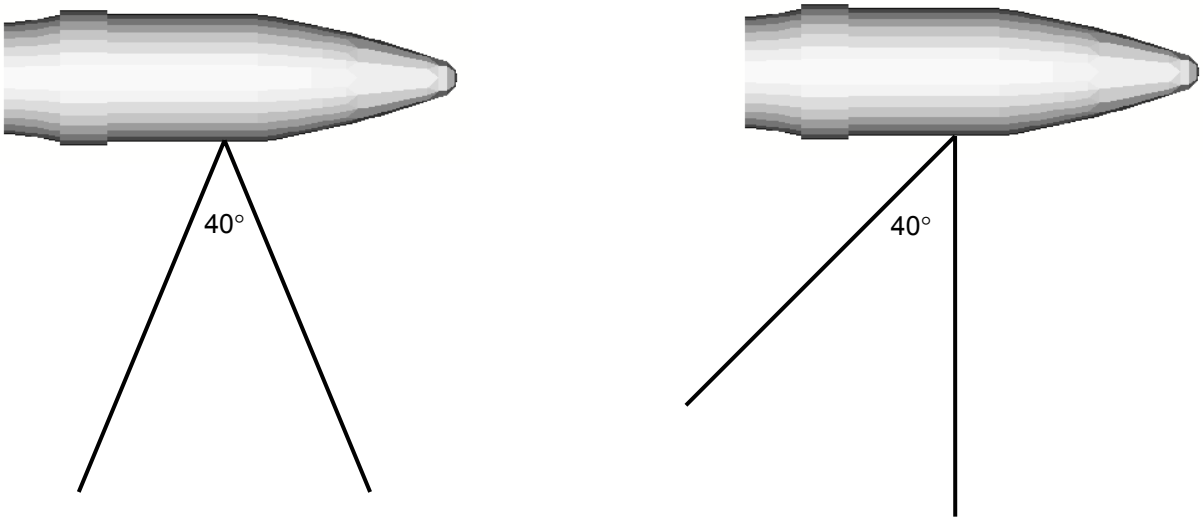

Figure 12. Target Imaged Around Broadside (left) **and with a 20-Degree Offset** (right) **for a Notional 40° Integration Angle.**

Table 7. Comparison of Measured and Modeled Broadside and Offset Average RCS.

	155-mm projectile			500-lb bomb			2,000-lb bomb		
	Measured	**-20:20**	**-40:0**	**Measured**	**-20:20**	**-40:0**	**Measured**	**-20:20**	**-40:0**
HH	- 9.9	- 6.7	- 8.2	0.4	5.9	2.2	5.7	9.4	6.4
HV	-19.4	-23.2	-19.2	-18.0	-22.4	-20.0	-11.5	-22.4	-22.2
VV	-10.6	- 8.6	-10.0	-4.5	- 0.7	- 2.9	- 3.3	2.0	- 0.3

4.4 TECHNOLOGY COMPARISON

It was not the intent of this study to do a comparison between the FOPEN ATD radar and existing technology. However, a ground-based SAR system that is comparable to the FOPEN SAR is the mobile BoomSAR system (designed and constructed by ARL). It allows data collection over a wide range of varying clutter and target-in-clutter scenarios to support

phenomenology and target discrimination research [3]. The BoomSAR emulates the collection geometries that can be achieved by a radar mounted on a helicopter, or unmanned aerial vehicle (Figure 13). This radar covers 20-1,100 MHz and the full polarization matrix to accomplish this task. The radar is mounted atop a 150-ft telescoping boom lift that can be driven forward while fully erect to permit the collection of synthetic aperture radar data (Figure 14). This setup allows the system to emulate the imaging geometry of either an airborne or vehicle mounted radar. Further, it provides a high degree of control in the design and execution of test scenarios. The BoomSAR uses an impulse waveform with spectral response extending from 20 MHz to more than 1 GHz. This 1-GHz bandwidth, which is directly digitized on receive, gives a measured 6-inch resolution in the range dimension. High resolution in the cross-range dimension is achieved with the use of SAR techniques to process those returns to achieve resolution as small as 11 inches.

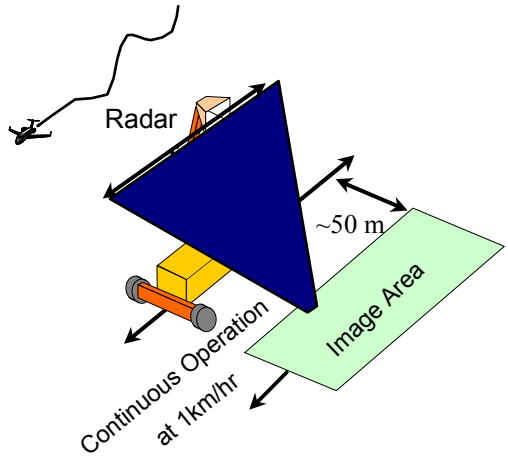

Figure 13. BoomSAR Collection Geometry.

Figure 14. ARL BoomSAR system.

This page left blank intentionally.

5.0 COST ASSESSMENT

5.1 COST REPORTING

This project did not involve the development of technology so no capital, operational, or maintenance costs were incurred. The UXO demonstration flights represented a small, incremental portion of a large deployment under the DARPA program, which bore the costs of logistics, mobilization, and demobilization. The minimum cost for a single flight of the FOPEN SAR system is approximately $150,000. There was a flat fee for usage of the FOPEN SAR system of $10,000 per flight that included five passes and processed imagery of each pass. Ground truth costs are estimated at $40,000. Advanced image processing was provided by MIT/LL at a cost of approximately $20,000 per pass, providing four images per pass. Recent improvements in image processing have likely eliminated the need for the additional processing by MIT/LL, making the flight cost $100,000 or less.

5.2 COST ANALYSIS

Not applicable.

5.3 COST COMPARISON

Not applicable.

This page left blank intentionally.

6.0 IMPLEMENTATION ISSUES

6.1 COST OBSERVATIONS

Not applicable.

6.2 PERFORMANCE OBSERVATIONS

Since the objective of this project was to measure the signature of select UXO items using the FOPEN SAR system, there were no pre-set criteria. The study showed that a low frequency, limited bandwidth SAR system was capable of imaging isolated items the size of a 500-lb bomb and clustered targets the size of 155-mm in an uncluttered environment. Combining multiple-look angles improves detection. It also enforced suspicions that a limited frequency bandwidth is not sufficient for detecting smaller targets. The image modeling suggests that a combination of features, such as frequency response, polarization, and aspect angle, may allow separation of UXO from clutter. The restriction on digging at Camp Navajo still leaves the question as to whether an airborne SAR system can image buried UXO.

6.3 SCALE-UP

Not applicable.

6.4 OTHER SIGNIFICANT OBSERVATIONS

The FOPEN SAR system was not designed for the detection of ordnance-size items. The system bandwidth is designed for detecting large tactical vehicles under foliage.

6.5 LESSONS LEARNED

Large targets (bomb-size) and dense collections of smaller (155-mm) targets can be detected by the UHF FOPEN SAR when located on the ground surface in sparsely vegetated areas. Multiple aircraft headings will likely increase the chance of imaging UXO. Trees proximate to targets degraded the target resolution and no targets under foliage were able to be resolved. An airborne SAR system with greater resolution is desirable. A combination of frequency, polarization, and angle-dependent scattering features may allow separation of UXO from clutter when the UXO has a reasonable length-to-diameter ratio and is still basically intact. To determine their usefulness, more work is needed in exploiting effective combinations of these features in automatic detection algorithms. With the modeling software and image processing techniques now available, studies should be conducted to determine a set of SAR system parameters that would be applicable for detecting UXO in various terrain conditions.

6.6 END-USER ISSUES

Not applicable.

6.7 APPROACH TO REGULATORY COMPLIANCE AND ACCEPTANCE

This project had no direct involvement with regulators or the public.

7.0 REFERENCES

1. L.A. Bessette. 2002. *FOPEN ATD Camp Navajo UXO Data Collection Summary.* Massachusetts Institute of Technology Lincoln Laboratory, Project Report FPR-22, 4 June 2002.

2. L. Carin. 2002. *Duke Final Report on ESTCP SAR Project.* Department of Electrical and Computer Engineering, Duke University, 2002.

3. A. Sullivan, K. Kappra, and M. Ressler. 2002. *Electromagnetic Model Predictions of the Unique Frequency, Angle, and Polarization Dependent Signatures of Unexploded Ordnance.* U.S. Army Research Laboratory, 2002.

4. Simms, J.E. 2002. *Applications of Synthetic Aperture Radar (SAR) to UXO Delineation.* U.S. Army Engineer Research and Development Center, Vicksburg, MS. 2002.

5. A.F. Yegulalp. 1999. *Fast Backprojection Algorithm for Synthetic Aperture Radar*. Proc. 1999 IEEE Int. Radar Conf., 60–65, 20–22 April 1999, Waltham, Mass.

6. L.M. Novak and M.C. Burl. *Optimal Speckle Reduction in Polarimetric SAR Imagery*. IEEE Trans. Aerosp. Elec. Sys., March 1990.

This page left blank intentionally.

APPENDIX A

POINTS OF CONTACT

Point of Contact	Organization	Phone/Fax/E-mail	Role in Project
Janet Simms	U.S. Army Engineer Research and Development Center Geotechnical and Structures Laboratory 3909 Halls Ferry Road Vicksburg, MS 39180-6199	(601) 634-3493 (601) 634-3453 simmsj@wes.army.mil	Project Manager
Lawrence Carin	Department of Electrical & Computer Engineering Duke University Box 90291 Durham, NC 27708-0291	(919) 660-5270 (919)660-5293 lcarin@ee.duke.edu	Algorithm Development/Model Generation
Karl Kappra	U.S. Army Research Laboratory ATTN AMSRL SE RU 2800 Powder Mill Road Adelphi, MD 20783	(301) 394-0848 (301) 394-4690 kkappra@arl.army.mil	Image Modeling
Serpil Ayasli	MIT Lincoln Laboratory Room: S3–431 244 Wood Street Lexington, MA 02420-9185	(781) 981-7440 (781) 981-0300 serpil@ll.mit.edu	Image Processing

ESTCP Program Office

901 North Stuart Street
Suite 303
Arlington, Virginia 22203

(703) 696-2117 (Phone)
(703) 696-2114 (Fax)

e-mail: estcp@estcp.org
www.estcp.org